SYNAPSE 45:259–269 (2002)

Differential Distribution of PDE4D Splice Variant mRNAs in Rat Brain Suggests Association With Specific Pathways and Presynaptical Localization

XAVIER MIRÓ,[1] SILVIA PÉREZ-TORRES,[2] PERE PUIGDOMÈNECH,[1] JOSÉ M. PALACIOS,[2†] AND GUADALUPE MENGOD[2*]

[1]*Department of Molecular Genetics, Instituto de Biología Molecular de Barcelona, CID-CSIC, E-08034 Barcelona, Spain*

[2]*Department of Neurochemistry, Institut d'Investigacions Biomèdiques de Barcelona, CSIC (IDIBAPS), Barcelona E-08036, Spain*

KEY WORDS in situ hybridization; emesis; area postrema; depression; serotonergic cells; rolipram

ABSTRACT cAMP plays an important role as a second-messenger molecule controlling multiple cellular processes. Its hydrolysis provides an important mechanism by which cAMP levels are regulated. This is performed by a large multigene family of cyclic nucleotide phosphodiesterases (PDEs). Members of the PDE4 enzyme family are selectively inhibited by rolipram. Five different mRNA splice forms for PDE4D have been isolated. Here, we analyzed the regional distribution of the mRNAs coding for the splice variants PDE4D1, PDE4D2, PDE4D3, PDE4D4, and PDE4D5 in the rat brain by in situ hybridization histochemistry using specific radiolabeled oligonucleotides. We found that all five splice variants showed a distinct distribution pattern and, in some cases, in association with specific brain pathways. The most relevant differences were in hippocampal formation, medial habenula, basal ganglia, and area postrema, at both the regional and cellular level. The dorsal and median raphe nuclei exclusively contained PDE4D2 mRNA transcripts, probably located on serotonergic cells. PDE4D1 mRNA was expressed in some white matter cells. PDE4D1 and PDE4D2 mRNA splice forms presented a similar distribution in the area postrema, whereas for PDE4D4 and PDE4D5 the cellular distribution presented a complementary pattern. The differential expression of PDE4D mRNA splice variants in the area postrema is consistent with their possible involvement in emesis control and suggests new molecular targets for a more selective drug design. **Synapse 45:259–269, 2002.**

INTRODUCTION

Cyclic nucleotide phosphodiesterases (PDEs) are classified into 12 families on the basis of their substrate specificity, kinetic properties, inhibitor sensitivity, and amino acid sequences (Conti and Jin, 1999; Fawcett et al., 2000; Soderling and Beavo, 2000; Houslay, 2001). These PDE families can be further distinguished according to their ability to hydrolyze cAMP or cGMP or both. cAMP-specific PDE4s differ from other PDEs in the catalytic domain sequence (Houslay et al., 1998) and by their specific inhibition by rolipram. It is composed of four members (PDE4A, PDE4B, PDE4C, and PDE4D) whose genes have been found to be expressed in many brain regions (Beavo, 1995; Cherry and Davis, 1999; Iwahashi et al., 1996; Perez-Torres et al., 2000) and with additional diversity being generated by alternative mRNA splicing or by the use of alternative promoters (Houslay et al., 1998). PDE4 enzymes are characterized by the presence of highly conserved blocks of sequence, UCR1 and UCR2, located immediately N-terminal to the catalytic unit (Bolger et al., 1993; Hous-

Contract grant sponsor: Fundació La Marató de TV3; Contract grant number: 1017/97; Contract grant sponsor: CICYT; Contract grant numbers: SAF1999-0123, 2FD97-0395.

†Current address for José M. Palacios: Research Center, Almirall Prodesfarma S.A., Cardener 68-74, E-08024 Barcelona, Spain.

*Correspondence to: Guadalupe Mengod, PhD, Department of Neurochemistry IIBB-CSIC (IDIBAPS), Rosselló 161 6 floor, Barcelona 08036, Spain. E-mail: gmlnqr@iibb.csic.es

Received 29 January 2002; Accepted 16 April 2002

DOI 10.1002/syn.10100

lay et al., 1998). The so-called "long" PDE4 isoenzymes contain both UCR1 and UCR2, whereas the "short" isoforms lack UCR1 and have either an intact or N-terminally truncated UCR2 form. UCR1 and UCR2 do not share sequence similarity with each other and are separated by a region of relatively low similarity (Bolger et al., 1993; Houslay et al., 1998). Five different spliced forms for PDE4D have been characterized (Bolger et al., 1993, 1997; Sette et al., 1994; Nemoz et al., 1996) all of which appear to be conserved among mammals (Jin et al., 1998). The short PDE4D isoforms are PDE4D1 and PDE4D2 and the long isoforms are PDE4D3, PDE4D4, and PDE4D5 (Bolger et al., 1993; Houslay et al., 1998). They all show specific intracellular locations (Jin et al., 1998), expression patterns (Miro et al., 2000), activation (Vicini and Conti, 1997), and isoform-specific interactions with other proteins (Beard et al., 1999; Yarwood et al., 1999; Steele et al., 2001; Verde et al., 2001).

Rolipram increases the intracellular availability of cAMP by selective inhibition of PDE4 (Davis, 1984). In clinical trials rolipram has shown antidepressant activity (Wachtel, 1983; Wachtel and Schneider, 1986; Scott et al., 1991) but its use is hampered by a high incidence of nausea and vomiting (Hebenstreit et al., 1989). The mechanism by which PDE4 inhibition results in increased vomiting and nausea in dog and human (Hebenstreit et al., 1989; Heaslip and Evans, 1995) is not fully understood, but probably includes both central and peripheral sites of actions. The presence of mRNAs coding for PDE4B and PDE4D in the area postrema (Perez-Torres et al., 2000), a region which is known to mediate these effects (Borinson and Wang, 1953; Carpenter et al., 1988), suggests that cAMP signaling modification in this area could be involved in the emetic effects of PDE4 inhibitors. In the present work we performed a detailed regional and cellular distribution for each one of the five PDE4D splice variants in the rat brain by in situ hybridization histochemistry.

MATERIALS AND METHODS

Animals

Adult male Wistar rats (200–300 g) were purchased from Iffa Credo (Lyon, France). Animal care followed Spanish legislation on "Protection of animals used in experimental and other scientific purposes" in agreement with the European (E.E.C) regulations (O.J. of E.C. L358/1 18/12/1986). Animals were killed by decapitation, brains were quickly removed, frozen on dry ice, and kept at −20°C. Tissue sections 14 μm thick were cut on a microtome-cryostat (Microm HM500 OM, Waldorf, Germany), thaw-mounted onto APTS (3-aminopropyltriethoxysilane; Sigma, St. Louis, MO) coated slides, and kept at −20°C until used.

Hybridization probes

Oligonucleotide probes were complementary either to the common amino-terminal region of the PDE4D splice variants (the catalytic domain being avoided) to detect all isoforms or to unique regions of each PDE4D splice variant. The oligonucleotides used were complementary to the following base sequences (GenBank accession number in brackets): PDE4D, bases 1586–1630 [U09456]. For the short PDE4D variants, 40-mer oligonucleotides were designed that were complementary to the junction sequences arising from the two possible exon combinations (see fig. 1 in Bolger et al., 1997) PDE4D1, bases 180–219 [U09455]; PDE4D2, bases 117–163 [U09456]. For the long PDE4D variants, since they differ at their 5′ end, 45-mers were designed that were complementary to unique regions for each splice form upstream of the common UCR1 domain: PDE4D3, bases 1–45 [U09457]; PDE4D4, bases 360–404 [AF031373]; PDE4D5, bases 251–295 [AF012073]. They were custom-synthesized by Amersham Pharmacia Biotech (UK).

The oligonucleotides were labeled at their 3′-end by using [α-^{32}P]dATP (3000 Ci/mmol; New England Nuclear, Boston, MA) and terminal deoxynucleotidyltransferase (Roche Molecular Biochemicals, Mannheim, Germany) at a final specific activity of $0.8–1.2 \times 10^4$ Ci/mmol. Labeled probes were purified through QIAquick Nucleotide Removal columns (Qiagen, Germany).

In situ hybridization histochemistry

Frozen tissue sections were brought to room temperature, air-dried, and fixed for 20 min in 4% paraformaldehyde in phosphate-buffered saline (1× PBS: 2.6 mM KCl, 1.4 mM KH_2PO_4, 136 mM NaCl, 8 mM Na_2HPO_4), washed once in 3× PBS, twice in 1× PBS, 5 min each, and incubated in a freshly prepared solution of predigested pronase (Calbiochem, San Diego, CA) at a final concentration of 24 U/ml in 50 mM Tris-HCl pH 7.5, 5 mM EDTA for 2 min at room temperature. Proteolytic activity was stopped by immersion for 30 sec in 2 mg/ml glycine in PBS. Tissues were rinsed in PBS and dehydrated in ethanol 70 and 100%, 2 min each. For hybridization, labeled probes were diluted to a final concentration of approximately $1.5–2 \times 10^7$cpm/ml in a solution containing 50% formamide, 4× SSC (1× SSC: 150 mM NaCl, 15 mM sodium citrate), 1× Denhardt's solution (0.02% Ficoll, 0.02% polyvinylpyrrolidone, 0.02% bovine serum albumin), 1% sarkosyl, 10% dextran sulfate, 20 mM phosphate buffer, pH 7.0, 250 μg/ml yeast tRNA, and 500 μg/ml salmon sperm DNA. Tissues were covered with 100 μl of the hybridization solution and overlaid with Nescofilm (Bando Chemical, Kobe, Japan) coverslips to prevent evaporation. Sections were incubated in humid boxes overnight at 42°C and then washed 4 times (45 min each) in 600 mM NaCl, 20 mM Tris-HCl, pH 7.5, 1 mM EDTA at 60°C.

Hybridized sections were exposed to β-max film (Amersham, UK) for 3–5 weeks at −70°C with intensifying screens.

The oligonucleotide probes used in this study were complementary to a region of the PDE4D mRNA that shares few similarities with the members of this family and the five PDE4D splice variants, thus minimizing the possibility of unspecific cross-hybridization. The specificity of the oligonucleotide hybridization signals was assessed in different ways: for a given oligonucleotide probe the presence of a 50-fold excess of the same unlabeled oligonucleotide in the hybridization buffer resulted in an abolishment of the specific hybridization signal (data not shown). The thermal stability of the hybrids was examined by washing a series of consecutive hybridized sections at increasing temperatures: specific hybridization signals were still present in sections washed at 70°C but they were completely absent from sections washed at 80°C. No such decrease was observed in the background levels of the signal (data not shown). The hybridization pattern obtained for each of the five probes is clearly distinct among them and also from those obtained with probes for other PDEs (Perez-Torres et al., 2000; Miro et al., 2001). RT-PCR amplification with splice variant-specific primers for each PDE 4D isoform was performed with mRNA extracted from different cell lines. The resulting bands of the expected size hybridized with the corresponding oligonucleotide probe (Miro et al., 2000). The short PDE4D variant 40-mer probes were designed in such a way that a 20 basepair region common for both PDE4D1 and PDE4D2 forms was contained in each oligonucleotide. According to our previously published experience (Sola et al., 1993), in the stringent hybridization conditions in which the experiments were performed, there will be no hybridization signal coming from the labeled 20-mer probes.

Duplicates of the hybridized sections were dipped in nuclear track Hypercoat LM-1emulsion (Amersham Pharmacia Biotech) to determine cellular localization of the hybridized probes. Slides were exposed for 5 weeks and developed in D19 (Kodak, Rochester, NY) at 20°C. Sections were examined using bright- and dark-field light microscopy (Leitz, Laborlux S, Wetzlar, Germany). For anatomical reference, adjacent sections were stained with cresyl violet. Brain areas and nuclei were identified according to Paxinos and Watson (1998).

RESULTS

The distribution of PDE4D1, PDE4D2, PDE4D3, PDE4D4, and PDE4D5 mRNA splice variants visualized by in situ hybridization histochemistry at different coronal levels of the rat brain showed a heterogeneous pattern (Fig. 1, Table I). The hybridization signal patterns obtained were compared to those for PDE4D mRNA. Abundant levels of PDE4D2, PDE4D4, and PDE4D5 mRNA expression were detected in different neuronal populations. PDE4D1 mRNA was present in the pontine nuclei and in fiber tracts of the corpus callosum. In contrast, PDE4D3 mRNA was almost absent in many brain areas except in the olfactory bulb and ventral posterior thalamic nucleus.

In situ hybridization histochemistry provides reliable information concerning the relative abundance of a given mRNA in different regions. However, caution must be taken in comparing the relative hybridization signals produced by different probes that detect different mRNAs. In addition to the actual abundance of the different mRNAs, the intensity of the hybridization signals observed can be affected by other factors, such as differences in the hybridization efficiency of the various probes or differences in the specific activities of the probes. Therefore, the results presented here have to be interpreted with this caveat in mind when comparing the abundance of the mRNAs coding for the different PDE4D splice forms.

Cerebral cortex

The frontal cortex showed high levels of PDE4D2 mRNA, background levels of PDE4D3 and intermediate levels of the other PDE4D splice variants (Fig. 1A). A differential distribution pattern was observed for all the PDE4D splice variants in the frontoparietal cortex. PDE4D2 mRNA levels were high in layer IV (Figs. 1B1 and 4) similar to PDE4D mRNA (Figs. 1B0 and 4). PDE4D4 mRNA was more abundant in layer VI and PDE4D5 mRNA in layers III and VI (Figs. 1B5 and 4). Low levels of PDE4D1 were observed across the layers (Figs. 1B1 and 4). PDE4D3 mRNA presented background hybridization levels (Figs. 1B3 and 4).

The intensity of the hybridization signal decreased in the anterior cingulate cortex for PDE4D2, PDE4D4 and PDE4D5 mRNAs (Fig. 1B2, B4, B5) and for PDE4D1 and PDE4D4 mRNAs in the posterior cingulate cortex (Fig. 1C1, C4). The levels of PDE4D3 and PDE4D5 mRNAs increased moderately in the retrospenial cortex (Fig. 1D3, D5).

Olfactory system

The mRNAs of the five PDE4D variants were found at high levels in the olfactory bulb (Fig. 1A1–A5). PDE4D2 mRNA was clearly the predominant splice variant present in the olfactory system, with high levels in the anterior olfactory nucleus, olfactory tubercle, and piriform cortex (see Figs. 1A2, 1B2, 3I), and low in the islands of Calleja. PDE4D3 and PDE4D4 mRNAs were not detected in the olfactory tubercle.

Basal ganglia and related areas

In caudate-putamen and accumbens nuclei PDE4D1 and PDE4D2 mRNA expression was low, corresponding to the levels of PDE4D mRNA. In substantia nigra,

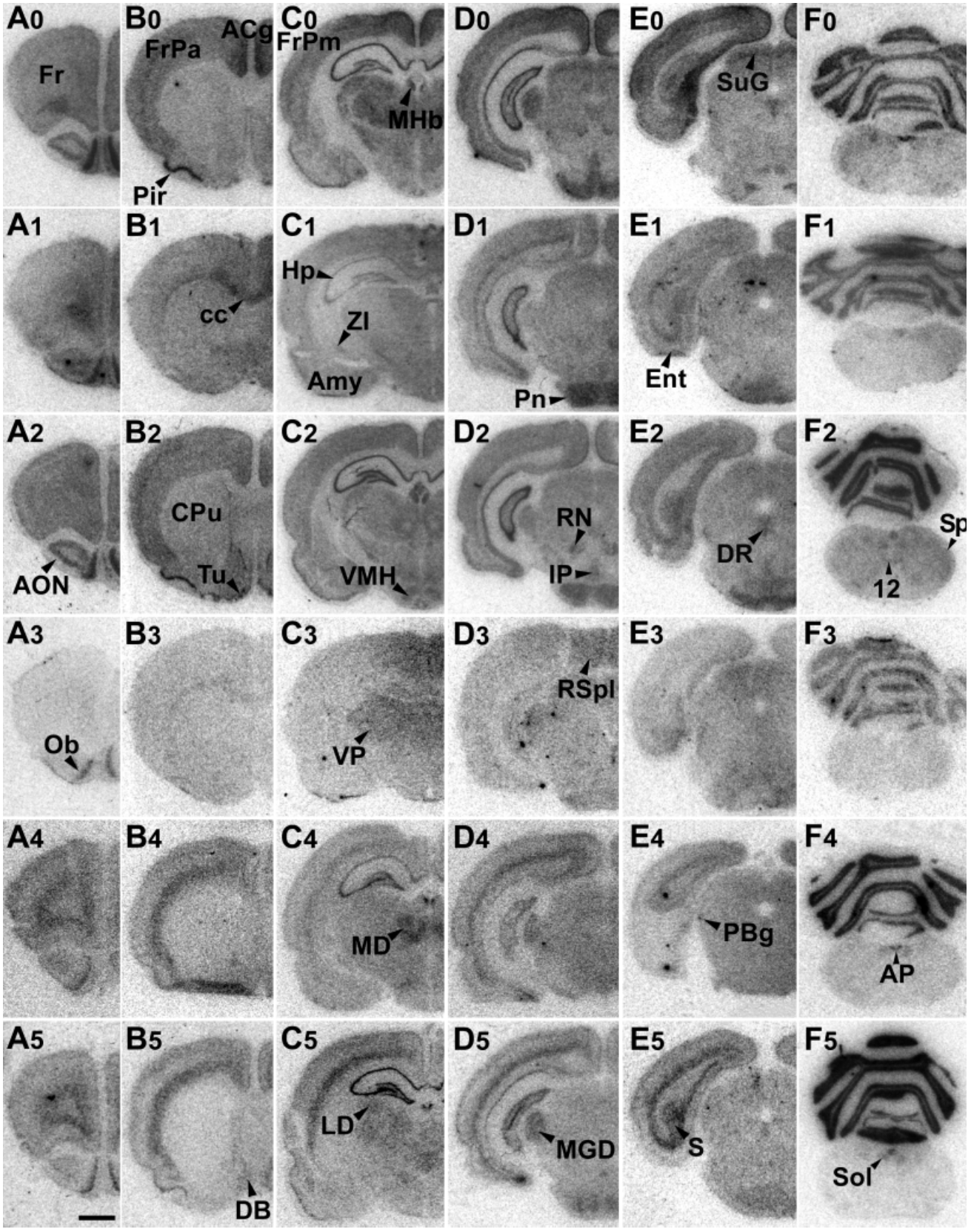

Fig. 1. Regional distribution of PDE4D splice variant mRNAs in rat brain. **A–F** are film autoradiograms showing hybridization patterns obtained with the ^{32}P-labeled oligonucleotides complementary to PDE4D (*0*), PDE4D1 (*1*), PDE4D2 (*2*), PDE4D3 (*3*), PDE4D4 (*4*), and PDE4D5 (*5*) mRNAs. Coronal brain sections are presented from **A–F** in a rostrocaudal progression. Bar = 2 mm. Hypoglossal nucleus (12), amygdala (Amy), anterior cingulate cortex (ACg), anterior olfactory nucleus (AON), area postrema (AP), corpus callosum (cc), caudate-putamen (Cpu), diagonal band (DB), dorsal raphe (DR), entorhinal cortex (Ent), frontal cortex (Fr), frontoparietal cortex (FrPa and FrPm), hippocampal formation (Hp), interpeduncular nuclei (IP), laterodorsal thalamic nucleus (LD), mediodorsal thalamic nucleus (MD), medial geniculate nucleus (MGD), medial habenular nucleus (MHb), olfactory bulb (Ob), parabigeminal nucleus (PBg), piriform cortex (Pir), pontine nuclei (Pn), red nucleus (RN), retrospenial cortex (RSpl), subiculum (S), nucleus of the solitary tract (Sol), nucleus of the spinal tract of the trigeminus (Sp), superficial gray layer of superior colliculus (SuG), olfactory tubercle (Tu), ventromedial hypothalamic nucleus (VMH), ventral posterior thalamic nucleus (VP), zona incerta (ZI).

TABLE I. Summary of PDE4D mRNA expression of the splice variants in the rat brain by in situ hybridization histochemistry; comparison with ^{3}H-rolipram binding sites

Brain area	PDE4D	PDE4D1	PDE4D2	PDE4D3	PDE4D4	PDE4D5	^{3}H-Rolipram*
Cerebral cortex							
Frontal cortex	+	+	+	−	+	+	+
Cingulate cortex	+	+	+	−	+	+	+
Frontoparietal cortex	+	+	+	−	+	+	+
Retrospenial cortex	+	+	+	+	+	+	+
Olfactory system							
Anterior olfactory nucleus	+	+	+	−	+	+	+
Olfactory bulb	+	+	+	+	+	+	+
Olfactory tubercle	+	+	+	−	−	+	+
Piriform cortex	+	−	+	−	+	+	+
Basal ganglia and related areas							
Genus corpus callosum	−	+	−	+	+	−	+
Caudate-Putamen	+	+	+	−	−	−	+
Accumbens nucleus	+	+	+	−	−	−	+
Amygdala	+	+	+	−	+	−	+
Substantia nigra	+	+	+	−	−	−	+
Septum and Hippocampal formation							
Septal nuclei	+	+	+	−	+	+	+
Ammon's horn							
pyramidal cells in CA1	+	+	+	−	+	+	+
pyramidal cells in CA2	+	+	+	+	+	+	+
pyramidal cells in CA3	+	+	+	−	+	+	+
hilus	+	+	+	−	+	+	+
Dentate gyrus	+	+	+	+	+	+	+
Subiculum	+	+	+	−	−	+	+
Entorhinal cortex	+	+	+	−	−	−	+
Diencephalon							
Laterodorsal thalamic nucleus	+	+	+	+	+	+	+
Mediodorsal thalamic nucleus	+	+	+	+	+	+	+
Medial habenular nucleus	+	+	+	−	+	+	+
Zona incerta	+	+	+	−	−	−	+
Lateral habenular nucleus	−	+	+	−	+	−	+
Ventroposterior thalamic nuclei	+	+	+	+	+	+	+
Medial geniculate body	+	+	+	+	+	+	+
Ventromedial hypothalamus	+	+	+	−	−	−	+
Brainstem							
Superior colliculus	+	+	+	+	+	+	+
Red nucleus	+	+	+	−	−	−	+
Principal oculomotor nerve	+	−	+	−	−	−	−
Interpeduncular nuclei	+	+	+	−	−	−	+
Pontine nuclei	+	+	+	+	+	+	+
Dorsal raphe	+	−	+	−	−	−	+
Parabigeminal nucleus	+	−	−	−	+	−	+
Facial nucleus	+	−	+	−	−	−	+
Dorsal cochlear nuclei	+	+	+	+	−	−	+
Nucleus of the solitary tract	+	−	+	−	+	+	+
Vestibular nuclei	+	+	+	+	−	−	+
Spinal trigeminal nucleus	+	−	+	−	−	−	+
Hypoglossal nucleus	+	−	+	−	−	−	−
Area postrema	+	+	+	−	+	+	+
Cerebellum							
Cerebellum granular cell layer	+	+	+	+	+	+	+
Cerebellar nuclei	+	−	+	−	−	−	+

+. signal; present; − no detectable signal.
*Pérez-Torres et al. (2000).

PDE4D2 mRNA was observed in the pars compacta, and PDE4D1 mRNA in the pars reticulata (Fig. 1D2, D1). In the genus corpus callosum, the expression levels were high for PDE4D1, intermediate for PDE4D4, and low for PDE4D3 mRNAs (Fig. 1B1, B4, B3). Low PDE4D1, PDE4D2, and PDE4D4 mRNA hybridization signals were present in the amygdala.

Septum and hippocampal formation

Low expression was observed in the septum for the PDE4D splice variants. Whereas PDE4D2 and PDE4D5 mRNAs were seen in the lateral septal nucleus, PDE4D1 mRNA was the only form present in the medial septal nucleus. (Fig. 1B).

Marked differences in the pattern of expression were also observed in the hippocampal formation (Figs. 1C, 2). A comparatively high expression for PDE4D5 and PDE4D2 and low for PDE4D4 could be observed, PDE4D3 being almost absent. All five forms were present in the pyramidal cell layer of the CA2 field (Fig. 2). PDE4D2 and PDE4D5 mRNA displayed high hybridization signal in hilus and granule cell layer of the dentate gyrus (Fig. 2B,E). Low and intermediate levels of PDE4D1 and PDE4D2 mRNAs were observed in the entorhinal cortex and subiculum, respectively (Fig. 1D1, D2). In the latter area PDE4D5 mRNA could also be visualized (Fig. 1D5). In presubiculum and parasubiculum, low levels of PDE4D2 mRNA were detected.

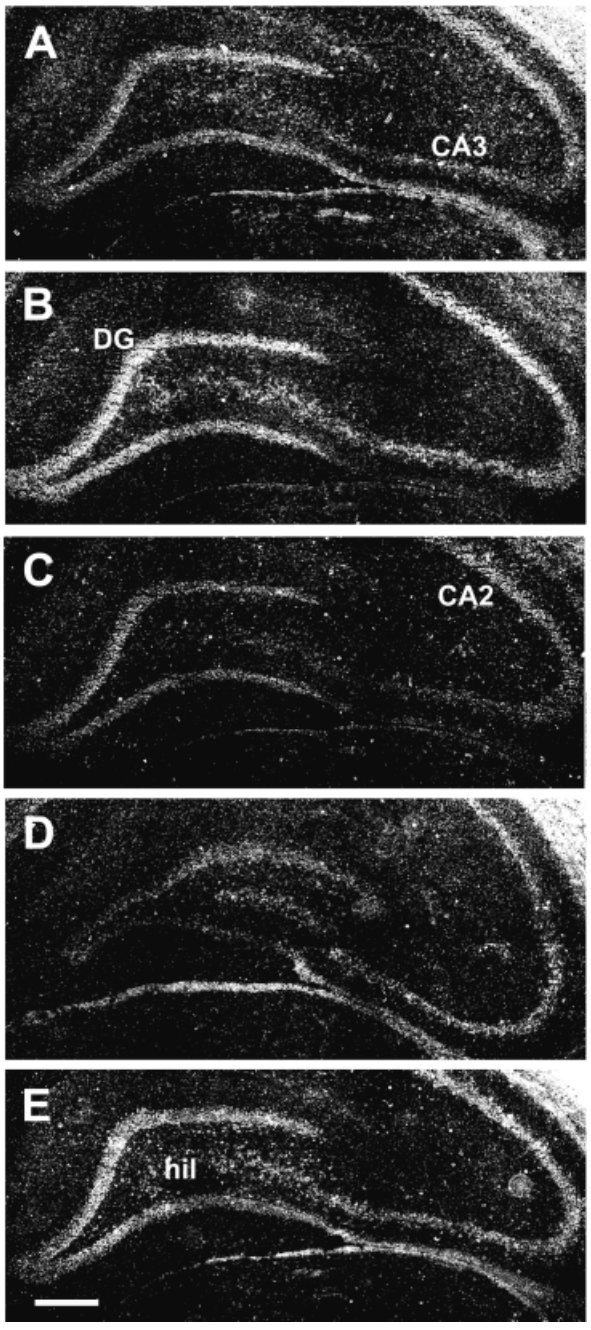

Fig. 2. Cellular expression of PDE4D splice variant mRNAs in the hippocampal formation. Autoradiographic images are presented as dark-field photomicrographs from emulsion-dipped tissue sections in which autoradiographic grains are seen as bright points. While PDE4D3 (**C**) mRNA was only present in the CA2 field (CA2) and dentate gyrus (DG), the other PDE4D splice variant mRNAs were also present in the CA3 fields (CA3) and hilus (hil). PDE4D4 (**D**) mRNA showed low intensity in the dentate gyrus, where PDE4D2 (**B**) and PDE4D5 (**E**) were clearly enriched. PDE4D1 (**A**) mRNA presented the higher intensity in the CA2 field. Bar = 0.2 mm.

Diencephalon

Strong hybridization signals for PDE4D4 and PDE4D5, intermediate for PDE4D2, and low for PDE4D1 mRNAs were seen in the medial habenular nucleus (Fig. 1C), with a differential distribution pattern. Whereas PDE4D4 mRNA expression was restricted to the upper portion of the medial habenular nucleus (Fig. 3C), PDE4D5 mRNA was found in the ventral two-thirds of this nucleus (Fig. 3D). In contrast, PDE4D1 and PDE4D2 mRNA were homogeneously distributed in both parts (Fig. 3A,B). Weak hybridization signals for PDE4D1, PDE4D2, and PDE4D4 mRNA were detected in the lateral habenular nucleus. PDE4D3 mRNA was absent in the habenula.

In the medial geniculate body, whereas PDE4D4 and PDE4D5 mRNA transcripts were detected at high intensity, the other PDE4D splice variants displayed low or intermediate hybridization signal (Fig. 1D1–D5). Intermediate levels of PDE4D1 and PDE4D2 mRNAs were seen in the zona incerta. PDE4D splice variants were detected at different intensities in different thalamic nuclei, except in the central medial and intermediodorsal thalamic nuclei, in agreement with the distribution observed for PDE4D mRNA (Fig. 1C0). Noteworthy is the almost exclusive expression of PDE4D3 in some thalamic nuclei (Fig. 1C3). PDE4D1 and PDE4D2 mRNAs were detected at intermediate levels in the ventromedial hypothalamus nucleus (Fig. 1C1, C2)

Brainstem

PDE4D2 mRNA was the only splice form detected in the dorsal and median raphe nuclei (Figs. 1E2 and 3L). In the red and interpeduncular nuclei where PDE4D was present (Fig. 1D0), PDE4D2 was observed (Figs. 1D2, 3K) at intermediate levels, whereas PDE4D1 mRNA was visualized but at lower densities (Fig. 1D1). All PDE4D splice variants were expressed at low or intermediate densities in the superficial gray layer of superior colliculus (Fig. 1E1–E5) and also in the pontine nuclei (Fig. 1D1–D5), although displaying different intensities.

In the hypoglossal nucleus and principal oculomotor nerve PDE4D2 mRNA was the only splice variant visualized. Interestingly, in the area postrema the expression was high for PDE4D1 (Fig. 3E) and PDE4D4 (Fig. 3G) and weak for PDE4D2 (Fig. 3F) and PDE4D5 (Fig. 3H) mRNAs. PDE4D3 mRNA transcripts were not detected.

In both facial (not shown) and spinal trigeminal nuclei, PDE4D2 was the only splice variant visualized (Fig. 1F2). In the parabigeminal nucleus only PDE4D4 mRNA could be detected (Fig. 1E4). PDE4D4 and PDE4D5 were absent in the dorsal cochlear nucleus, whereas PDE4D1 and PDE4D3 mRNAs were present at low and PDE4D2 mRNA at intermediate densities. In addition, low hybridization signals for PDE4D2 mRNA were detected in the dorsal motor nucleus of the vagus. Likewise, PDE4D2, PDE4D4 and PDE4D5 mRNAs were present at low levels in the nucleus of the solitary tract.

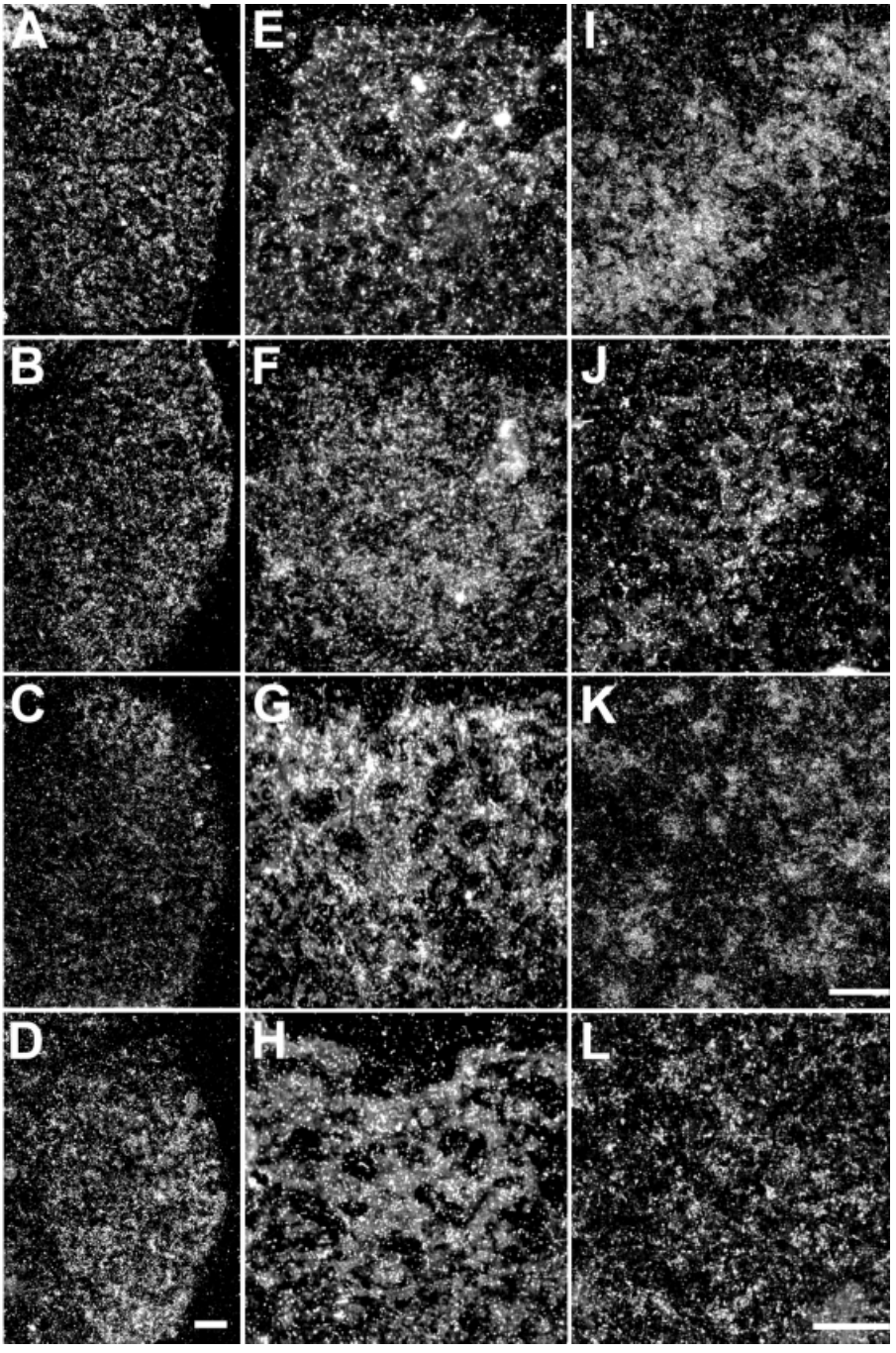

Fig. 3. Cellular localization of some of the PDE4D splice variant mRNAs in the medial habenular nucleus (**A–D**), area postrema (**E–H**), olfactory tubercle (**I–J**), red nucleus (**K**), and dorsal raphe (**L**). **A–L** are dark-field photomicrographs from emulsion-dipped sections. While PDE4D1 (**A**) and PDE4D2 (**B**) mRNAs were found in the entire medial habenular nucleus, PDE4D4 (**C**) mRNA expression was restricted to the upper area and PDE4D5 (**D**) mRNA to the ventral two-thirds of the medial habenular nucleus. PDE4D1 (**E**), PDE4D2 (**F**), PDE4D4 (**G**), and PDE4D5 (**H**) mRNAs were detected in the area postrema. PDE4D2 (**I**) mRNA was clearly enriched in the olfactory tubercle, where PDE4D5 (**J**) mRNA was also present. PDE4D2 mRNA was also detected in the red nucleus (**K**) and dorsal raphe (**L**). Bars = 50 μm **A–J, K, L**.

Cerebellum

All PDE4D splice variants were present in the cerebellum at intermediate (PDE4D1, PDE4D3, and PDE4D4) or high (PDE4D2 and PDE4D5) intensities, with the hybridization signal, like that observed for PDE4D mRNA (Fig. 1F0), restricted to the granule cell layer. In the cerebellar nuclei, PDE4D3 mRNA was present at low densities, PDE4D2 mRNA at intermediate densities, and PDE4D4 and PDE4D5 mRNAs were absent.

DISCUSSION

The aim of the present work was to determine the regional and cellular distribution in the rat brain of the five splice variants of PDE4D by using oligonucleotide probes that selectively recognize each of the five alternatively spliced transcripts of PDE4D. Our results show that the mRNA expression of the splice forms presents a differential distribution pattern, mainly in neurons but also in white matter cells. The summation

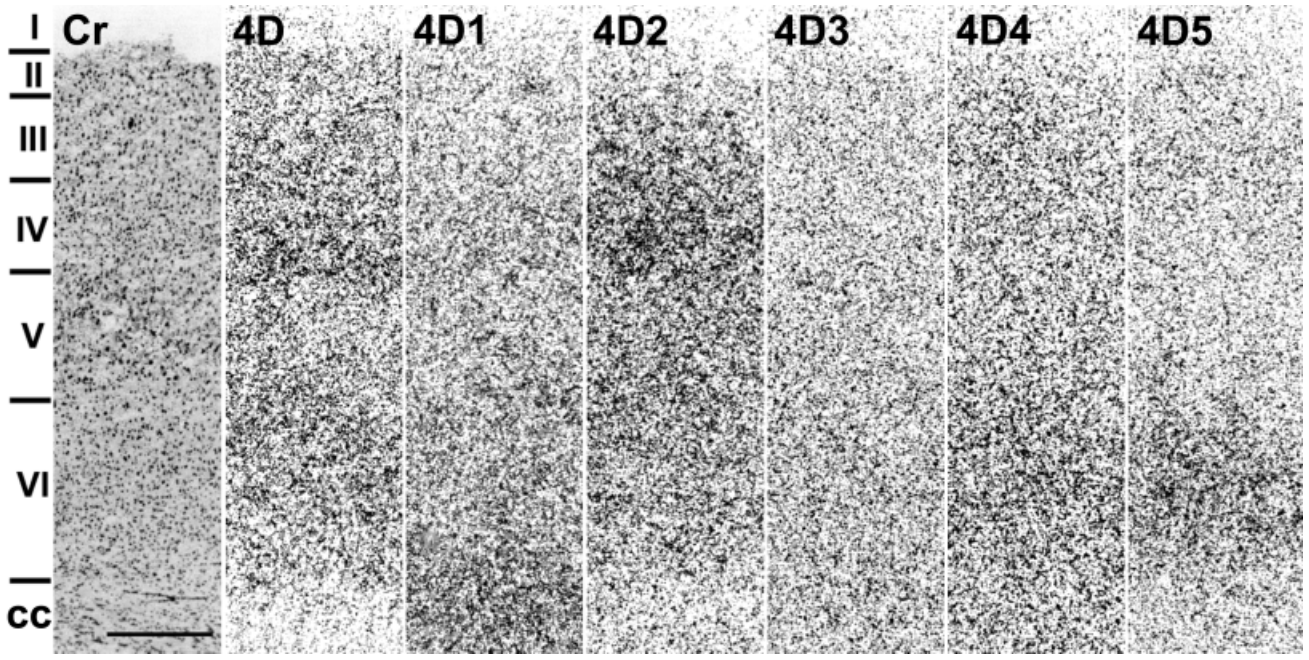

Fig. 4. Distribution of the mRNAs coding for PDE4D and the five splice variants in the neocortex. PDE4D1 (*4D1*) and PDE4D2 (*4D2*) mRNAs are more enriched in layers IV and VI. On the contrary, PDE4D4 (*4D4*) and PDE4D5 (*4D5*) mRNAs show a higher hybridization in the layer VI. PDE4D3 (*4D3*) mRNA presents, in general, low density. Note the strong hybridization signal of PDE4D1 in the corpus callosum (cc). The first panel (*Cr*) is a cresyl violet-stained section consecutive with the others. Bar = 0.5 mm.

of their regional distribution agrees, in general, with that observed for PDE4D mRNA .

The evidence for the presence at specific areas in rat brain of the five PDE4D splice variants is only indirect. Their expression in brain has been demonstrated by immunoblot (Bolger et al., 1997), on total rat brain homogenates, in agreement with our data. By immunoprecipitation of several dissected rat brain areas, a PDE4D residual activity can be identified in the work of McPhee et al. (1995) which is, in general, in agreement with the distribution for PDE4D presented in our work. In contrast, other authors (Iona et al., 1998; Takahashi et al., 1999) have shown that PDE4D1 and PDE4D2 are absent in cortex and cerebellum homogenates with different antibodies. Our results thus show the presence of PDE4D splice variant mRNAs at different expression levels and locations in rat brain, thus supporting the idea of isoform-specific properties and roles in particular cAMP pathways (Beard et al., 1999; Yarwood et al., 1999; Miro et al., 2000). We have identified some brain areas where only PDE4D1 and PDE4D2 mRNA are detected. These two PDE4D splice variants are called "short forms" since they lack the upstream conserved region UCR1, a putative regulatory domain with a phosphorylation site (Hoffmann et al., 1998). PDE4D1 and PDE4D2 have been found to exist only in the cytosol of rat brain homogenates, whereas the three long form splice variants were found in both cytosolic and particulate fractions (Bolger et al., 1997). We observed a PDE4D short form-specific expression in the entorhinal cortex, reticular thalamic nucleus, zona incerta, ventromedial hypothalamus, and red nucleus. It is known that the red nucleus receives input from hypothalamic areas, thalamic nuclei, and zona incerta (Paxinos, 1995), as well as cerebral cortex and cerebellar nuclei, areas where PDE4D1 and PDE4D2 mRNA were also detected. Entorhinal cortex receives direct olfactory bulb inputs and projects to the dentate gyrus of hippocampus, as well as indusium griseum, where low levels of PDE4D2 mRNA are detected. These olfactory-entorhinal-hippocampal circuits may be important for establishment of olfactory memories formed or associated with other events. This is a relevant point due to the fact that PDE4 family is the mammalian equivalent of the *dunce* gene of *Drosophila melanogaster*, implicated in learning and memory (Davis et al., 1995).

A clear differential distribution pattern has been observed in the medial habenula: PDE4D1 and PDE4D2 mRNAs are homogeneously expressed, PDE4D3 mRNA is absent, PDE4D4 mRNA is restricted to the upper area, and PDE4D5 mRNA is enriched in the ventral two-thirds. Most neurons in this area express choline acetyltransferase (Woolf and Butcher, 1985). This zone has been assigned as the inferior part of the medial habenula (Andres et al., 1999), which projects to the more caudal parts of the central and intermediate interpeduncular subnuclei (Kawaja et al., 1988). PDE4D4 transcripts are restricted to the upper area assigned as superior part of the medial habenula (Andres et al., 1999), which in turns contains substance P-immunoreactive neurons.

Terminal fields positive for substance P are largely restricted to the lateral subnucleus of the interpeduncular nucleus, which receives projections from the superior part of the medial habenula (Andres et al., 1999). This suggests that PDE4D4 could be associated with neurons containing substance P as neurotransmitter, whereas PDE4D5 could be related to the cholinergic system as well as PDE4D1 and PDE4D2. Immunohistochemical studies in the mouse brain (Cherry and Davis, 1999), using antibodies against PDE4A, PDE4B, and PDE4D, have shown a high level of expression of PDE4D protein in all the components of the habenulo-interpeduncular pathway: the medial habenula, fasciculus retroflexus, and interpeduncular nucleus. When compared with our in situ hybridization results in rat, these data suggest that the PDE4D4 and PDE4D5 could be expressed in different cell populations of the medial habenula and transported through the fasciculus retroflexus to the interpeduncular nucleus, where they could be localized presynaptically in the terminals of the habenular neurons. The habenulo-interpeduncular pathway thus offers an interesting model where the role of different splice forms of the PDE4D family as regulators of intracellular cAMP concentration can be analyzed.

PDE4D2 was the only splice variant expressed in the dorsal and median raphe nuclei. This confirms our previous work (Perez-Torres et al., 2000), where we described PDE4D as the only PDE4 isozyme expressed in the raphe nuclei of the rat, in contrast with the results from Iwahashi et al. (1996), reporting PDE4A and PDE4B expression in raphe. Since PDE4D2 is found in these raphe nuclei it may participate in the regulation of the activity of serotonergic neurons.

Recently, the distribution has been published of some splice variants for another phosphodiesterase 4, PDE4A (McPhee et al., 2001), in rat brain. There were some areas displaying a differential expression for the long and short forms of PDE4A. One of these areas was the cerebellum, where only the short PDE4A1 isoform was present. This contrasts with our data, since all five PDE4D variants, short and long isoforms, are expressed at relatively high levels in the granular cell layer of the cerebellum. This observed difference could have a functional significance for cAMP signaling in the central nervous system, especially when considering that PDE4D but not PDE4A isoforms are regulated by ERK phosphorylation (McPhee et al., 2001; Hoffmann et al., 1999; MacKenzie et al., 2000; Baillie et al., 2000). Furthermore, no PDE4A long isoforms are found in the CA3 layer at some levels of the hippocampal formation (McPhee et al., 2001), whereas the five PDE4D splice forms are present in all CA fields, with the exception of PDE4D3 (a long form), which is absent in CA1. This could be an important point, especially since PDE4D3 interacts with PKA type II and are assembled via a common protein kinase A-anchoring protein, AKAP450, in Sertoli cells of the testis (Tasken et al., 2001) and in heart tissue via a muscle-selective A-kinase anchoring protein, mAKAP (Dodge et al., 2001).

The PDE4-specific inhibitor rolipram, used for the treatment of endogenous depression (Wachtel, 1983), exhibits antidepressant effects in models predictive of antidepressant activity (Wachtel and Schneider, 1986) and it has been shown to be clinically effective (Zeller et al., 1984; Scott et al., 1991). However, its side effects (nausea, pyrosis, and emesis) (Horowski and Sastre-y-Hernandez, 1985), represent a significant drawback for its clinical application. An immunohistochemical study in the mouse brain (Cherry and Davis, 1999) revealed strong PDE4D, but not PDE4A or PDE4B, immunoreactivity in the neuropil of the area postrema and nucleus of the solitary tract. Our data indicates that four of the five PDE4D splice forms are expressed in the area postrema, whereas low expression was seen for three of them in the nucleus of the solitary tract. This, together with the previously described presence of the mRNA coding for PDE4B (Takahashi et al., 1999; Perez-Torres et al., 2000) in the area postrema and nucleus of the solitary tract, is of great relevance due to the fact that this region is known to be involved in emesis (Borinson and Wang, 1953; Carpenter et al., 1988), suggesting that cAMP signaling modulation in this area could mediate the emetic effects of PDE4 inhibitors.

Besides rolipram, other selective PDE4 inhibitors have been studied, mainly for the treatment of asthma, as well as for other chronic inflammatory diseases such as arthritis, chronic obstructive pulmonary disease (COPD), atopic dermatitis, and multiple sclerosis (MS) (Giembycz, 2000; Souness et al., 2000). The clinical data available for compounds such as cilomilast and roflumilast (both without a particular isoform selective profile) show the presence of nausea and vomiting as well as headache and other central effects, even if at a different degree of intensity. Several other PDE4 inhibitors appear to be in clinical development, although their isoform selectivity is unknown. The availability of isoform-selective PDE4 inhibitors is an important requirement to establish the role of these forms in the regulation of cAMP levels in cell functions.

Other central and peripheral effects have been described after administration of PDE4 inhibitors: regulation of the inflammatory function in many cells and prevention, delay, and reduction of the clinical severity of experimental allergic encephalomyelitis, a rat model of multiple sclerosis (Sommer et al., 1995; Martinez et al., 1999). The presence of some PDE4D splice forms in white matter cells described in the present work deserves further investigation. There are also studies on the inhibition by rolipram of LPS-induced expression of TNF-α in the rat brain (Buttini et al., 1997). This could be related to the effects of PDE4 regulation on TNF-α

levels which are postulated to be involved in multiple sclerosis and Alzheimer's disease. Also described is a reduction of neuronal damage by rolipram following cerebral ischemia in the gerbil (Kato et al., 1995) and in Alzheimer's disease (McGeer et al., 1990; McGeer and McGeer, 1995).

It has been speculated that each PDE isozyme plays different roles related to the fine-tuning of intracellular levels of cAMP that could be related to their different Km for cAMP and, thus, to variations in intracellular cAMP levels. Inactivation of one PDE should produce a loss of function. Flies deficient in the *Drosophila melanogaster dunce* PDE (homolog of the mammalian PDE4D) display impairments in the central nervous system and reproductive functions (Dudai et al., 1976). Mice with a targeted disruption of the PDE4D gene survive and reproduce, although they are less fertile and with a reduced body weight (Jin et al., 1999). In these knockout mice, a marked decrease in the rolipram-sensitive PDE activity was reported in the pituitary gland, cerebellum, and ovary when compared with wild-type animals (Jin et al., 1999). The airways of these mice are no longer responsive to cholinergic stimulation (Hansen et al., 2000). The lung phenotype of the PDE4D-deficient mice demonstrates that this gene plays a nonredundant role in cAMP homeostasis. Therefore, it would appear that other PDE isoenzymes are not upregulated due to the absence of PDE4D splice variants in these mice, supporting the idea that each PDE could have unique and nonoverlapping functions in cell signaling. This is an important point for the development of PDE4 isozyme-specific inhibitors as therapeutic agents.

In conclusion, our studies have shown for the first time that PDE4D splice variants PDE4D1, PDE4D2, PDE4D3, PDE4D4, and PDE4D5 present a distinct regional and cellular distribution in rat brain, suggesting that the presence of PDE4D splice variants could play distinct functions by differential regulation of the intracellular cAMP concentration. In this work, we have identified areas in the rat brain where the effects of brain lesions and pharmacological treatments could be studied. The development of specific inhibitors for each PDE4D splice variant should allow proof of their implication in different functions.

ACKNOWLEDGMENT

X.M. is a recipient of a fellowship from CIRIT (Centre de Referència of the Generalitat de Catalunya) and S.P.-T. from CIRIT (Generalitat de Catalunya).

REFERENCES

Andres KH, von During M, Veh RW. 1999. Subnuclear organization of the rat habenular complexes. J Comp Neurol 407:130–150.

Baillie GS, MacKenzie SJ, McPhee I, Houslay MD. 2000. Sub-family selective actions in the ability of Erk2 MAP kinase to phosphorylate and regulate the activity of PDE4 cyclic AMP-specific phosphodiesterases. Br J Pharmacol 131:811–819.

Beard MB, O'Connell JC, Bolger GB, Houslay MD. 1999. The unique N-terminal domain of the cAMP phosphodiesterase PDE4D4 allows for interaction with specific SH3 domains. FEBS Lett 460:173–177.

Beavo JA. 1995. Cyclic nucleotide phosphodiesterases: functional implications of multiple isoforms. Physiol Rev 75:725–748.

Bolger G, Michaeli T, Martins T, St.John T, Steiner B, Rodgers L, Riggs M, Wigler M, Ferguson K. 1993. A family of human phosphodiesterases homologous to the dunce learning and memory gene product of Drosophila melanogaster are potential targets for antidepressant drugs. Mol Cell Biol 13:6558–6571.

Bolger GB, Erdogan S, Jones RE, Loughney K, Scotland G, Hoffmann R, Wilkinson I, Farrell C, Houslay MD. 1997. Characterization of five different proteins produced by alternatively spliced mRNAs from the human cAMP-specific phosphodiesterase PDE4D gene. Biochem J 328:539–548.

Borinson HL, Wang SC. 1953. Physiology and pharmacology of vomiting. Pharmacol Rev 5:193–230.

Buttini M, Mir A, Appel K, Wiederhold KH, Limonta S, Gebicke-Haerter PJ, Boddeke HW. 1997. Lipopolysaccharide induces expression of tumour necrosis factor alpha in rat brain: inhibition by methylprednisolone and by rolipram. Br J Pharmacol 122:1483–1489.

Carpenter DO, Briggs DB, Knox AP, Strominger N. 1988. Excitation of area postrema neurons by transmitters, peptides, and cyclic nucleotides. J Neurophysiol 59:358–369.

Cherry JA, Davis RL. 1999. Cyclic AMP phosphodiesterases are localized in regions of the mouse brain associated with reinforcement, movement, and affect. J Comp Neurol 407:287–301.

Conti M, Jin SL. 1999. The molecular biology of cyclic nucleotide phosphodiesterases. Prog Nucleic Acid Res Mol Biol 63:1–38.

Davis CW. 1984. Assessment of selective inhibition of rat cerebral cortical calcium-independent and calcium-dependent phosphodiesterases in crude extracts using deoxycyclic AMP and potassium ions. Biochim Biophys Acta 797:354–362.

Davis RL, Cherry J, Dauwalder B, Han PL, Skoulakis E. 1995. The cyclic AMP system and Drosophila learning. Mol Cell Biochem 149-150:271–278.

Dodge KL, Khouangsathiene S, Kapiloff MS, Mouton R, Hill EV, Houslay MD, Langeberg LK, Scott JD. 2001. mAKAP assembles a protein kinase A/PDE4 phosphodiesterase cAMP signaling module. EMBO J 20:1921–1930.

Dudai Y, Jan YN, Byers D, Quinn WG, Benzer S. 1976. Dunce, a mutant of Drosophila deficient in learning. Proc Natl Acad Sci USA 73:1684–1688.

Fawcett L, Baxendale R, Stacey P, McGrouther C, Harrow I, Soderling S, Hetman J, Beavo JA, Phillips SC. 2000. Molecular cloning and characterization of a distinct human phosphodiesterase gene family: PDE11A. Proc Natl Acad Sci USA 97:3702–3707.

Giembycz M. 2000. PDE4D-deficient mice knock the breath out of asthma. Trends Pharmacol Sci 21:291–292.

Hansen G, Jin S, Umetsu DT, Conti M. 2000. Absence of muscarinic cholinergic airway responses in mice deficient in the cyclic nucleotide phosphodiesterase PDE4D. Proc Natl Acad Sci USA 97:6751–6756.

Heaslip RJ, Evans DY. 1995. Emetic, central nervous system, and pulmonary activities of rolipram in the dog. Eur J Pharmacol 286: 281–290.

Hebenstreit GF, Fellerer K, Fichte K, Fischer G, Geyer N, Meya U, Sastre, Schony W, Schratzer M, Soukop W. 1989. Rolipram in major depressive disorder: results of a double-blind comparative study with imipramine. Pharmacopsychiatry 22:156–160.

Hoffmann R, Wilkinson IR, McCallum JF, Engels P, Houslay MD. 1998. cAMP-specific phosphodiesterase HSPDE4D3 mutants which mimic activation and changes in rolipram inhibition triggered by protein kinase A phosphorylation of Ser-54: generation of a molecular model. Biochem J 333:139–149.

Hoffmann R, Baillie GS, MacKenzie SJ, Yarwood SJ, Houslay MD. 1999. The MAP kinase ERK2 inhibits the cyclic AMP-specific phosphodiesterase HSPDE4D3 by phosphorylating it at Ser579. EMBO J 18:893–903.

Horowski R, Sastre-y-Hernandez M. 1985. Clinical effects of the neurotropic selective cAMP phosphodiesterase inhibitor rolipram in depressed patients: global evaluation of the preliminary reports. Curr Ther Res 38:23–29.

Houslay MD. 2001. PDE4 cAMP-specific phosphodiesterases. Prog Nucleic Acid Res Mol Biol 69:249–315.

Houslay MD, Sullivan M, Bolger GB. 1998. The multienzyme PDE4 cyclic adenosine monophosphate-specific phosphodiesterase family: intracellular targeting, regulation, and selective inhibition by compounds exerting anti-inflammatory and antidepressant actions. Adv Pharmacol 44:225–342.

Iona S, Cuomo M, Bushnik T, Naro F, Sette C, Hess M, Shelton ER, Conti M. 1998. Characterization of the rolipram-sensitive, cyclic AMP-specific phosphodiesterases: identification and differential expression of immunologically distinct forms in the rat brain. Mol Pharmacol 53:23–32.

Iwahashi Y, Furuyama T, Tano Y, Ishimoto I, Shimomura Y, Inagaki S. 1996. Differential distribution of mRNA encoding cAMP-specific phosphodiesterase isoforms in the rat brain. Mol Brain Res 38:14–24.

Jin SL, Bushnik T, Lan L, Conti M. 1998. Subcellular localization of rolipram-sensitive, cAMP-specific phosphodiesterases. Differential targeting and activation of the splicing variants derived from the PDE4D gene. J Biol Chem 273:19672–19678.

Jin SL, Richard FJ, Kuo WP, D'Ercole AJ, Conti M. 1999. Impaired growth and fertility of cAMP-specific phosphodiesterase PDE4D-deficient mice. Proc Natl Acad Sci USA 96:11998–12003.

Kato H, Araki T, Itoyama Y, Kogure K. 1995. Rolipram, a cyclic AMP-selective phosphodiesterase inhibitor, reduces neuronal damage following cerebral ischemia in the gerbil. Eur J Pharmacol 272:107–110.

Kawaja MD, Flumerfelt BA, Hrycyshyn AW. 1988. Topographical and ultrastructural investigation of the habenulo-interpeduncular pathway in the rat: a wheat germ agglutinin-horseradish peroxidase anterograde study. J Comp Neurol 275:117–127.

MacKenzie SJ, Baillie GS, McPhee I, Bolger GB, Houslay MD. 2000. ERK2 mitogen-activated protein kinase binding, phosphorylation, and regulation of the PDE4D cAMP-specific phosphodiesterases. The involvement of COOH-terminal docking sites and NH2-terminal UCR regions. J Biol Chem 275:16609–16617.

Martinez I, Puerta C, Redondo C, Garcia-Merino A. 1999. Type IV phosphodiesterase inhibition in experimental allergic encephalomyelitis of Lewis rats: sequential gene expression analysis of cytokines, adhesion molecules and the inducible nitric oxide synthase. J Neurol Sci 164:13–23.

McGeer PL, McGeer EG. 1995. The inflammatory response system of brain: implications for therapy of Alzheimer and other neurodegenerative diseases. Brain Res Rev 21:195–218.

McGeer PL, McGeer E, Rogers J, Sibley J. 1990. Anti-inflammatory drugs and Alzheimer disease. Lancet 335:1037.

McPhee I, Pooley L, Lobban M, Bolger G, Houslay MD. 1995. Identification, characterization and regional distribution in brain of RPDE-6 (RNPDE4A5), a novel splice variant of the PDE4A cyclic AMP phosphodiesterase family. Biochem J 310:965–974.

McPhee I, Cochran S, Houslay MD. 2001. The novel long PDE4A10 cyclic AMP phosphodiesterase shows a pattern of expression within brain that is distinct from the long PDE4A5 and short PDE4A1 isoforms. Cell Signal 13:911–918.

Miro X, Casacuberta JM, Gutierrez-Lopez MD, de Landazuri MO, Puigdomenech P. 2000. Phosphodiesterases 4D and 7A splice variants in the response of HUVEC cells to TNF-alpha(1). Biochem Biophys Res Commun 274:415–421.

Miro X, Perez-Torres S, Palacios JM, Puigdomenech P, Mengod G. 2001. Differential distribution of cAMP-specific phosphodiesterase 7A mRNA in rat brain and peripheral organs. Synapse 40:201–214.

Nemoz G, Zhang R, Sette C, Conti M. 1996. Identification of cyclic AMP-phosphodiesterase variants from the PDE4D gene expressed in human peripheral mononuclear cells. FEBS Lett 384:97–102.

Paxinos G. 1995. The rat nervous system, 2nd ed. New York: Academic Press.

Paxinos G, Watson C. 1998. The rat brain in stereotoxic coordinates, Fourth edition, Academic Press.

Perez-Torres S, Miro X, Palacios JM, Cortes R, Puigdomenech P, Mengod G. 2000. Phosphodiesterase type 4 isozymes expression in human brain examined by in situ hybridization histochemistry and[3H]rolipram binding autoradiography. Comparison with monkey and rat brain. J Chem Neuroanat 20:349–374.

Scott AI, Perini AF, Shering PA, Whalley LJ. 1991. In-patient major depression: is rolipram as effective as amitriptyline? Eur J Clin Pharmacol 40:127–129.

Sette C, Vicini E, Conti M. 1994. The rat PDE3/IVd phosphodiesterase gene codes for multiple proteins differentially activated by cAMP-dependent protein kinase. J Biol Chem 269:18271–18274.

Soderling SH, Beavo JA. 2000. Regulation of cAMP and cGMP signaling: new phosphodiesterases and new functions. Curr Opin Cell Biol 12:174–179.

Sola C, Mengod G, Probst A, Palacios JM. 1993. Differential regional and cellular distribution of beta-amyloid precursor protein messenger RNAs containing and lacking the Kunitz protease inhibitor domain in the brain of human, rat and mouse. Neuroscience 53: 267–295.

Sommer N, Loschmann PA, Northoff GH, Weller M, Steinbrecher A, Steinbach JP, Lichtenfels R, Meyermann R, Riethmuller A, Fontana A. 1995. The antidepressant rolipram suppresses cytokine production and prevents autoimmune encephalomyelitis. Nat Med 1:244–248.

Souness JE, Aldous D, Sargent C. 2000. Immunosuppressive and anti-inflammatory effects of cyclic AMP phosphodiesterase (PDE) type 4 inhibitors. Immunopharmacology 47:127–162.

Steele MR, McCahill A, Thompson DS, MacKenzie C, Isaacs NW, Houslay MD, Bolger GB. 2001. Identification of a surface on the beta-propeller protein RACK1 that interacts with the cAMP-specific phosphodiesterase PDE4D5. Cell Signal 13:507–513.

Takahashi M, Terwilliger R, Lane C, Mezes PS, Conti M, Duman RS. 1999. Chronic antidepressant administration increases the expression of cAMP-specific phosphodiesterase 4A and 4B isoforms. J Neurosci 19:610–618.

Tasken KA, Collas P, Kemmner WA, Witczak O, Conti M, Tasken K. 2001. Phosphodiesterase 4D and protein kinase a type II constitute a signaling unit in the centrosomal area. J Biol Chem 276:21999–22002.

Verde I, Pahlke G, Salanova M, Zhang G, Wang S, Coletti D, Onuffer J, Jin SL, Conti M. 2001. Myomegalin is a novel protein of the golgi/centrosome that interacts with a cyclic nucleotide phosphodiesterase. J Biol Chem 276:11189–11198.

Vicini E, Conti M. 1997. Characterization of an intronic promoter of a cyclic adenosine 3',5'-monophosphate (cAMP)-specific phosphodiesterase gene that confers hormone and cAMP inducibility. Mol Endocrinol 11:839–850.

Wachtel H. 1983. Potential antidepressant activity of rolipram and other selective cyclic adenosine 3',5'-monophosphate phosphodiesterase inhibitors. Neuropharmacology 22:267–272.

Wachtel H, Schneider HH. 1986. Rolipram, a novel antidepressant drug, reverses the hypothermia and hypokinesia of monoamine-depleted mice by an action beyond postsynaptic monoamine receptors. Neuropharmacology 25:1119–1126.

Woolf NJ, Butcher LL. 1985. Cholinergic systems in the rat brain. II. Projections to the interpeduncular nucleus. Brain Res Bull 14:63–83.

Yarwood SJ, Steele MR, Scotland G, Houslay MD, Bolger GB. 1999. The RACK1 signaling scaffold protein selectively interacts with the cAMP-specific phosphodiesterase PDE4D5 isoform. J Biol Chem 274:14909–14917.

Zeller E, Stief HJ, Pflug B, Sastre. 1984. Results of a phase II study of the antidepressant effect of rolipram. Pharmacopsychiatry 17:188–190.